Effect of Beam Length on Bond-Dependent Coefficient (kb) value for GFRP reinforced beams

M. Talha Junaid[1*], *Nadia* Nassif[1], *Salah* Altoubat[1], *Mohamed* Maalej[1] *and Raghad* Awad[1]

[1]Department of Civil and Environmental Engineering, University of Sharjah, Sharjah, UAE

Abstract. This study investigates the influence of beam span length on the bond-dependent coefficient (k_b) for GFRP-reinforced concrete beams—a key parameter in predicting crack widths under service loads. Design codes such as ACI 440.1R and CSA S806 adopt a fixed k_b value (typically 1.4), based on limited experimental data, which may overlook the effects of span-dependent bond behavior. To examine this, six full-scale beams with spans of 1950 mm, 2500 mm, and 3050 mm were tested under four-point bending. Crack widths and FRP bar strains were recorded to calculate k_b values. Results showed a clear variation in k_b with span length: shorter spans yielded higher k_b values due to localized bond stress, while longer spans showed lower values associated with more uniform stress distribution. Although limited in scope, the results suggest a consistent trend between span length and k_b, indicating the possibility of developing correlations to estimate k_b values for longer spans from reduced-span tests. These findings support that further research with expanded datasets is recommended to establish generalized relationships for use in design and code calibration.

1 Introduction

The use of fiber-reinforced polymer (FRP) bars in reinforced concrete (RC) structures has seen significant growth due to their corrosion resistance, high tensile strength, and non-magnetic properties. GFRP is the most widely used FRP type in civil engineering applications due to its favorable balance of mechanical performance, corrosion resistance, ease of handling, and, most notably, its cost-effectiveness compared to other fiber types such as carbon or aramid However, unlike steel bars, the bond behavior between FRP and concrete is more complex due to the heterogeneity and linear-elastic nature of FRP materials. This bond governs the transfer of stress from concrete to the reinforcement, directly influencing serviceability parameters such as crack width and deflection. To capture this interaction, design codes including ACI 440.1R [1] and CSA S806 [2] introduce the bond-dependent coefficient (kb) to adjust crack width predictions. Despite its critical role, the kb factor has historically been derived from analogies with steel RC behavior or limited experimental datasets, leading to significant variability in recommended values and testing methodologies.

Experimental investigations over the past two decades have attempted to address this gap by directly measuring k_b values in full-scale beam tests under service-level loads. The bond

* Corresponding author: mjunaid@sharjah.ac.ae

behavior—and consequently the k_b value—is influenced by the type of fiber used, as variations in axial stiffness, surface texture, and thermal expansion affect the interfacial performance between the bar and the concrete matrix [3-6]. Among the most referenced works, El-Nemr et al. [3, 7] conducted an extensive series of tests on GFRP-reinforced beams, demonstrating that variables such as reinforcement ratio, bar diameter, and concrete strength greatly influence crack behavior and the resulting k_b values, which ranged widely from 0.46 to 2.09. These studies revealed that increasing the number of GFRP bars, especially beyond recommended configurations, can significantly reduce crack widths, potentially underestimating the actual k_b.

Similarly, Mehany et al. [6] evaluated GFRP beams with different surface textures—sand-coated and ribbed—and observed that ribbed bars provided better mechanical interlock, resulting in lower kb values (ranging from 0.79 to 1.10). Gouda et al. [9] explored grooved and ribbed GFRP bar surfaces and noted a similar trend: surface texture greatly affects stress transfer efficiency and cracking behavior, with kb values between 0.6 and 1.6. Meanwhile, Benzecry et al. [10] examined the role of reinforcement detailing and span length, showing that even within CSA-compliant setups, k_b values can vary from 0.88 to 1.34 due to differences in beam stiffness and strain distribution.

Other researchers have investigated GFRP alongside other FRP types to compare relative bond performance. For instance, Kassem et al. [4] reported GFRP kb values above 1.0, especially for sand-coated bars, while Mostafa et al. [5] found GFRP bars to produce higher kb than CFRP when tested in high-strength concrete beams. In contrast, Dong et al. [11] introduced intermediate steel reinforcement in their GFRP beams, which unintentionally reduced observed kb values (down to 0.42) by restricting crack widths, highlighting how non-standard reinforcement details can distort the assessment of true bond behavior. McCallum [12], one of the earliest adopters of CSA Annex S protocols, emphasized the importance of accurate strain and crack measurements and reported kb values from 0.75 to 1.47 for sand-coated GFRP.

Despite these efforts, the majority of studies adhere to the standard 3000 mm beam span recommended in CSA S806 and ACI 440.11-22, and few have examined whether shorter spans could yield comparably reliable kb values. Given the high costs, material demands, and logistical challenges of full-length beam testing, this highlights a significant gap in the current state of research. To address this issue, the present study investigates the influence of beam span length on the bond-dependent coefficient (kb) for GFRP-reinforced concrete beams. A total of six full-scale beams with three different spans (1950 mm, 2500 mm, and 3000 mm), were tested under four-point bending. All beams were designed to fail by concrete crushing, consistent with serviceability-focused design. The aim of this study is to assess whether shorter spans can yield accurate and consistent kb values, and to explore the feasibility of a scaled-down, resource-efficient testing protocol that remains compliant with existing code provisions.

2 Experimental program

2.1 Geometry and Testing setup

This experimental program was designed to evaluate the influence of beam span length on the bond-dependent coefficient (k_b) in full-scale GFRP-reinforced concrete beams. Six beams with identical geometry and reinforcement details were tested under four-point bending. Span length was the primary variable (1950 mm, 2500 mm, 3050 mm), where two duplicate beams were tested at each span to verify repeatability. All beams were over-reinforced to ensure

concrete crushing as the dominant failure mode, as per CSA S806 Annex S recommendations for k_b testing.

The tested beams featured varying cross-sectional dimensions, where the longest span had a cross-section of 200 mm × 300 mm, and the shorter spans (1950 mm and 2500 mm) were constructed with reduced dimensions of 170 mm × 255 mm. Longitudinal reinforcement consisted of two 10 mm diameter GFRP bars, placed in the tension zone with an effective depth of 270 mm. The reinforcement ratio ranged from 0.32% to 0.44%, depending on the concrete cover. As for the shear reinforcement, closed steel stirrups of 10 mm diameter were spaced at 90 mm. Stirrups were discontinued at the theoretical shear span limit, in line with CSA S806 Annex S. Beyond the shear span region, stirrups were discontinued, and two 10 mm diameter steel bars were placed at the top of the cross-section solely to support the cage. These bars were not bonded to the concrete and did not contribute to the structural performance of the beam. The reinforcement layout is shown in

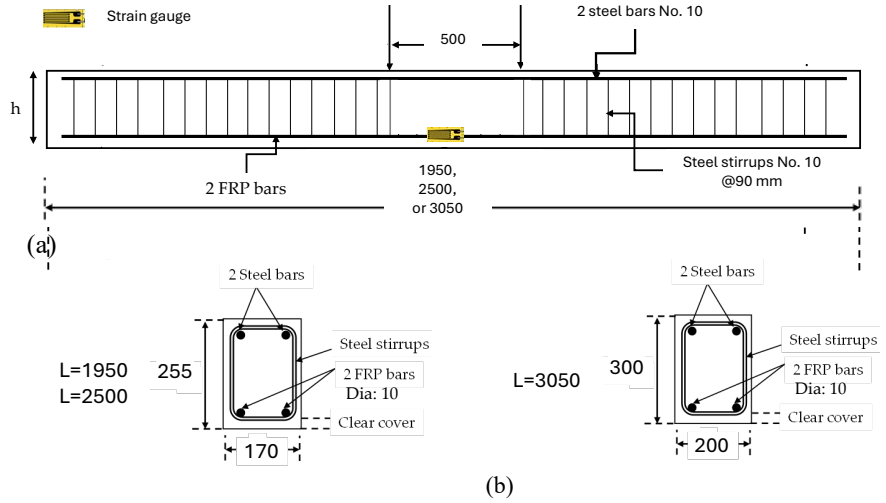

Fig. 1. (a) Details of FRP-RC beams in the KB testing program and reinforcement configuration, (b) Detail of the beams' cross-section. Each rebar was instrumented with a single strain gauge at midspan.

The k_b results will be collected and compared across the different beam sizes to identify trends in the k_b values, which will allow for the calibration of the smaller beam tests.

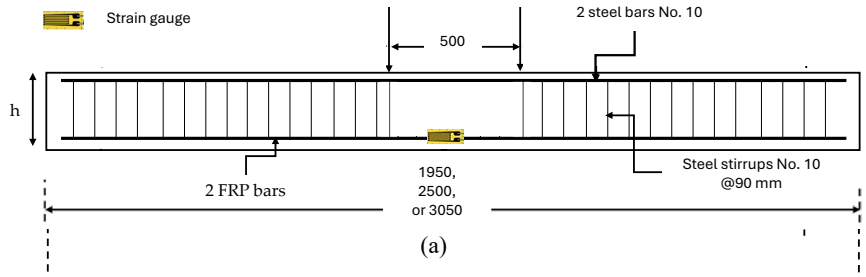

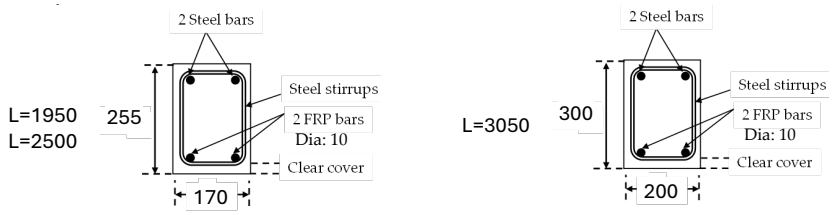

(b)

Fig. 2. (a) Details of FRP-RC beams in the KB testing program and reinforcement configuration, (b) Detail of the beams' cross-section.

All beams were simply supported and tested under four-point bending using the hydraulic actuator and a loading rate of 1.2 mm/min until failure or a crack width of 0.7 mm was reached. Loading was distributed through a steel spreader beam to create two equal point loads at one-third span. The overall test setup and instrumentation arrangement are shown in Fig. 3.

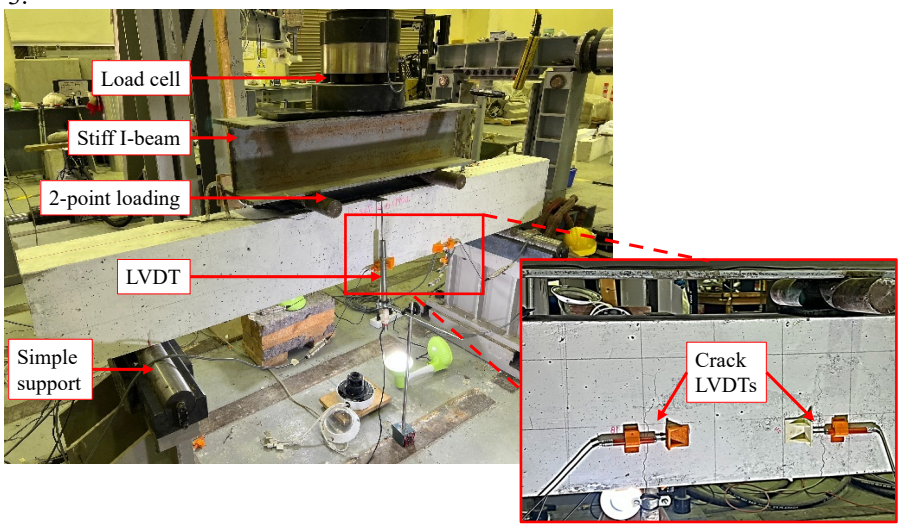

Fig. 3. Test setup and the placement of two LVDTs at first two cracks

3 Results and discussion

3.1 Cracking moment, flexural capacity and mode of failure

The cracking moments (M_{cr}) is identified at the onset of visible flexural cracking and reflected by reductions in stiffness in both moment–deflection and moment–strain responses. For the tested beams, M_{cr} was predicted using Equation (1), where the values ranged from 5.04 to 8.20 kN·m. The results demonstrated a clear dependence on the concrete compressive strength (f'_c), which governs the tensile capacity at cracking. Comparison with ACI 440.1R-15 predictions revealed an average experimental-to-predicted M_{cr} ratio of 0.91, revealing some level of over estimation—that is consistent with previously reported trends [8].

$$M_{cr} = \frac{f_r}{y_t} I_g \quad (1)$$

where I_g denotes the gross moment of inertia of uncracked section, y_t distance from centroid axis of cross-section to the extreme fiber in tension and the f_r represents the modulus of rupture, calculated following ACI 440.1R-15:

$$f_r = 0.62\sqrt{f_c'} \tag{2}$$

For the GFRP-reinforced concrete (FRP-RC) design, sections are typically over-reinforced, where the reinforcement ratio ρ_f is maintained above ρ_{fb}. This approach ensures that failure occurs through concrete crushing rather than sudden rupture of the FRP bars, resulting in a safer and more ductile failure mode. This design practice is recommended by major standards such as CSA S806 and ACI 440.11-22. The balanced reinforcement ratio (ρ_{fb}) represents the point where the compressive force in the concrete equals the tensile force in the FRP at failure. It depends on the strength of the concrete and the mechanical properties of the FRP bars and is calculated through Equations (3-4).

$$\rho_{fb} = \alpha_1\beta_1 \frac{f_c'}{f_{fu}} \frac{E_f\varepsilon_{cu}}{E_f\varepsilon_{cu} + f_{fu}} \tag{3}$$

$$\alpha_1 = 0.85;\ \beta_1 = 0.85 - 0.05(f_c' - 27.6)/6.9 \tag{4}$$

Crack patterns initiated as vertical flexural cracks at the tension face and inclined within the shear spans under combined stress conditions. Crack development stabilized at approximately $0.67M_{cr}$, with subsequent loading resulting primarily in the widening of existing cracks. An increase in reinforcement ratio ($\rho_f\ /\rho_{fb}$) led to a higher density of cracks and improved distribution. Table 1 summarizes the beams' properties and key parameters of the k_b testing program. All GFRP-reinforced beams of span ≤ 2500 mm in the study predominantly failed in compression due to concrete crushing, consistent with the expected behavior of over-reinforced section. This mode of failure occurred prior to yielding of the top steel reinforcement. The absence of stirrups in the constant moment region contributed to premature buckling of the top steel bars, which in turn led to spalling of the concrete at the compression face. An exception was observed for the long-span GFRP beam (G-10 at 3050 mm) with a relatively low reinforcement ratio ($\rho_f/\rho_{fb} = 1.01$), which exhibited a combined failure mode characterized by both concrete crushing and bar rupture. This indicates that even marginally over-reinforced long-span GFRP sections may be susceptible to brittle failure. The value of the axial stiffness is of interest in design equals 4335 kN. Fig. 4 shows the beams after testing for the various spans.

The comparison between experimental results and ACI 440.1R predictions in Table 2 and Fig. 5 revealed that the code tends to slightly underestimate the cracking moment (M_{cr}), with an average experimental-to-predicted ratio of 0.91. This aligns with trends observed in previous studies, where the ACI provisions yielded conservative estimates, particularly for GFRP-reinforced beams. In contrast, the predicted nominal moment capacities (M_n) showed better agreement, with an average ratio of 0.97, indicating that the ACI equations generally provide reasonable estimates for ultimate capacity. These findings suggest that while the ACI method remains suitable for design, slight underestimation of M_{cr} should be acknowledged, especially in serviceability evaluations.

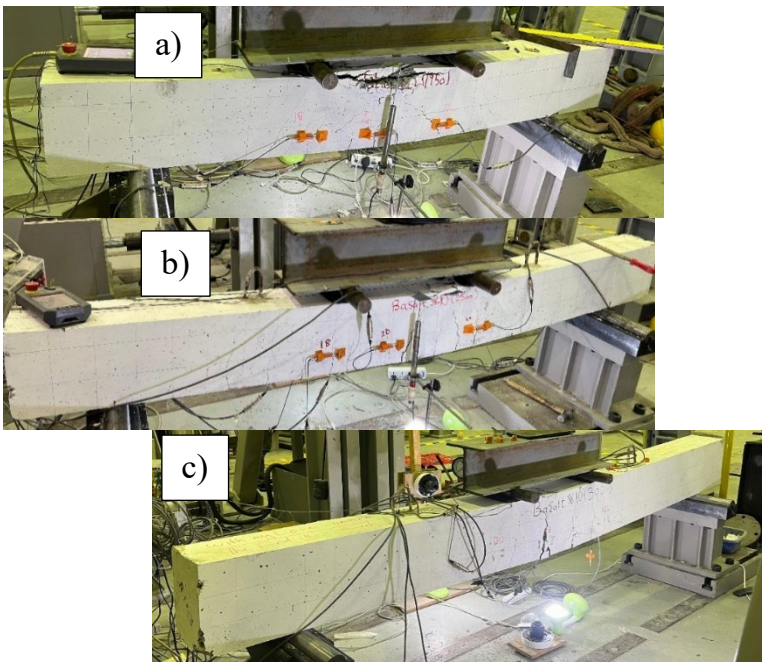

Fig. 4. Tested beams from: a) 1950mm, b) 2500mm and c) 3050 mm spans

Table 1. Testing program for GFRP-RC beams

Span (mm)	Beam	Replicate	f_c' (MPa)	f_t (MPa, ACI 318)	ρ_f (%)	ρ_b (%)	ρ_f/ρ_b
1950	G-10-1950	2	28.8	3.0	0.44%	0.30%	1.45
2500	G-10-2500	2	29.2	3.0	0.44%	0.31%	1.44
3000	G-10-3000	2	31.0	3.1	0.32%	0.32%	1.01

Table 2. Comparison of experimental and ACI predicted cracking moments and capacities

Beam	Replicate	Failure Mode*	Exp.		ACI		Ratio	
			M_{cr}	M_n	M_{cr}	M_n	$M_{cr\,(Exp)}/M_{cr\,(ACI)}$	$M_{n\,(Exp)}/M_{n\,(ACI)}$
			(kN.m)	(kN.m)	(kN.m)	(kN.m)	(kN.m)	(kN.m)
G-10-1950	1	C.C	5.95	23.6	5.96	25.09	1.00	0.94
	2	C.C	5.14	23.7			0.86	0.95
G-10-2500	1	C.C	5.04	24.8	5.74	24.87	0.88	1.00
	2	C.C	5.34	23.6			0.93	0.95
G-10-3050	1	C.C. + BR	7.76	32.0	9.06	34.39	0.86	0.93
	2	C.C. + BR	8.20	36.2			0.91	1.05
Average							**0.91**	**0.97**
std							**0.05**	**0.04**

* C.C = Concrete Crushing; BR = Bar Rupture

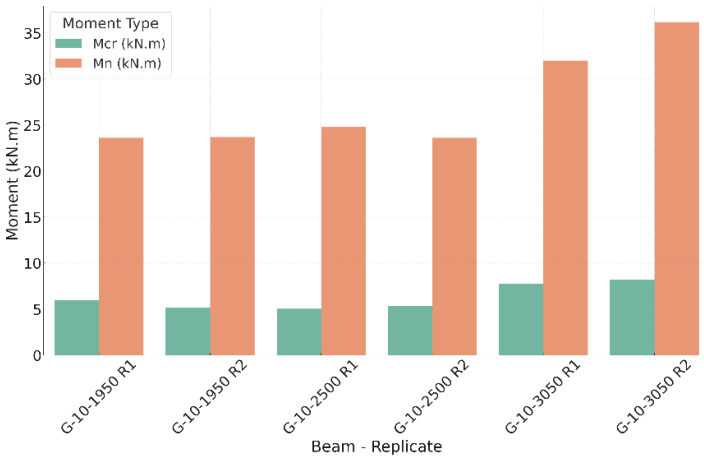

Fig. 5. Comparison of cracking and nominal capacity for the six tested GFRP beams

3.2 Crack patterns and behavior

The crack patterns observed in the tested GFRP beams reveal a strong correlation between beam span and crack distribution. Shorter beams (e.g., 1950 mm) exhibited frequent and closely spaced cracks, as shown in Fig 6a. This is attributed to high bond stress concentrations along the shorter embedment length, where the grooved surface texture of the GFRP bars intensifies local stress transfer at the bar–concrete interface. As the beam length increased, crack density notably decreased. In the 2500 mm beam (Fig 6b), fewer and more widely spaced cracks were observed. This trend continued in the 3050 mm beam (Fig 6c), which displayed the lowest number of cracks and the widest spacing, indicating more uniform stress distribution along the reinforcement. These observations align with findings by El-Nemr et al. [7], who reported that small-diameter GFRP bars in short spans tend to induce localized bond failures and high crack density. The current results reinforce the understanding that longer spans reduce bond stress concentrations, resulting in improved crack control.

To determine the bond-dependent coefficient k_b, a widely accepted approach is to back-calculate it from measured crack width and FRP bar strain using a rearranged version of the crack width formula adopted by ACI 440.1R and CSA S806. This method reflects the influence of bar-concrete bond characteristics under service load conditions and is expressed as:

$$k_b = \frac{w.E_f}{\varepsilon_f.s}$$

Where w is the measured crack width at service load, typically taken as 0.7 mm, E_f is the modulus of elasticity of the FRP reinforcement, ε_f is the measured strain in the FRP bar, s equals crack spacing.

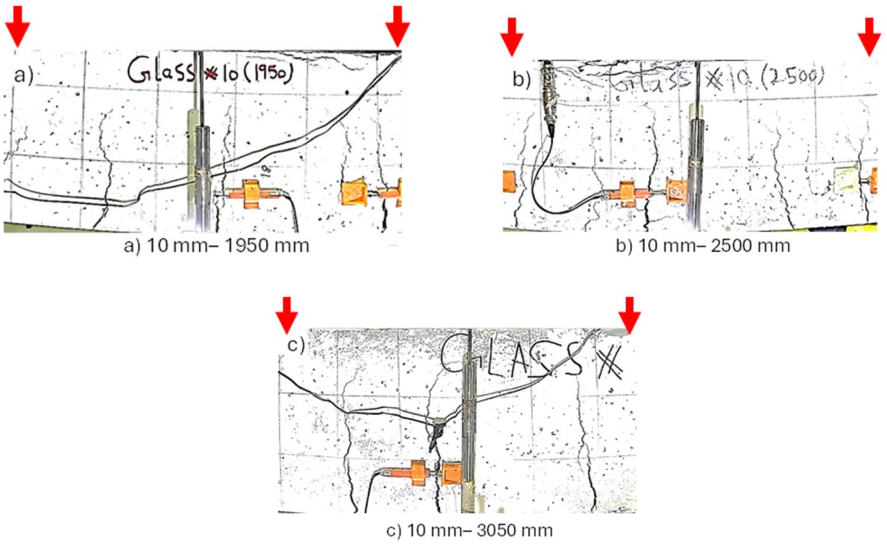

Fig 6. Crack patterns for GFRP-RC beams (diameter - length)

3.3 Comparison Analysis of the bond-dependent coefficient (k_b) with the literature

Among the key parameters influencing bond performance in FRP-reinforced concrete beams, clear span length plays a critical role in shaping the stress distribution and crack behavior used in the evaluation of the bond-dependent coefficient (k_b). The results of six GFRP-reinforced beams demonstrate a clear inverse relationship between span length and kb values. Beams with shorter spans (1950 mm and 2500 mm) exhibited higher k_b values, with averages of 1.39 and 1.03, respectively, while beams with the longest span (3050 mm) showed a significantly lower average k_b value of 0.76 (refer to Table 3). This trend is consistent with previous studies, such as Mehany et al. [6] and El-Nemr et al. [8], which found that shorter beams tend to concentrate bond stresses over a reduced embedment length, leading to increased crack widths and artificially elevated k_b values. The reduced span limits the ability of the reinforcement to distribute stresses effectively, thus intensifying local bond failures and producing higher measured k_b.

Conversely, longer beams (e.g., 3000 mm and above), as studied by Vincent et al. [13], and Kassem [14], provide more favorable conditions for stress redistribution along the bar length. In these cases, bond stresses are transferred more uniformly, resulting in lower k_b values and a more accurate representation of the long-term bond behavior of both GFRP and BFRP bars embedded in concrete.

Table 3. Macrostrains and k_b for tested FRP-RC beams

Beam	Microstrain		k_b		
	Bar 1	Bar 2	Bar1	Bar2	Average
G10-1950-S1	2962.2	3279.6	1.56	1.41	1.49
G10-1950-S2	3493.2	3764.4	1.33	1.23	1.28
G10-2500-S1	4656.3	4967.5	1.00	0.93	0.96
G10-2500-S2	4175.6	4292.7	1.11	1.08	1.10
G10-3050-S1	5287.6	5150.5	0.77	0.80	0.78
G10-3050-S2	5379.4	5789.6	0.76	0.71	0.73

4 Conclusion

This study confirms that beam span length has a significant effect on the bond-dependent coefficient (k_b) in GFRP-reinforced concrete beams. Shorter spans tend to produce higher kb values due to concentrated bond stress and localized cracking, potentially overestimating the severity of bond deficiencies. In contrast, longer spans promote more uniform bond stress transfer and yield lower kb values that more accurately reflect actual bond performance under service conditions. These findings validate the current code recommendations for large-scale testing, as prescribed by CSA S806 [1] and ACI 440.11 [2], for reliable k_b determination. However, with appropriate calibration, shorter-span tests may offer a practical and resource-efficient alternative for estimating k_b. By adjusting shorter-span results based on full-span reference values, accurate serviceability predictions can still be achieved. This approach has the potential to reduce testing demands while preserving the reliability needed for code-based design of FRP-reinforced structures.

References

1. ACI Committee 440, Guide for the Design and Construction of Structural Concrete Reinforced with FRP Bars, ACI 440.1R-15 (ACI, Farmington Hills, 2015)
2. CSA Group, Design and Construction of Building Components with Fibre-Reinforced Polymers, CSA S806-12 (CSA, Mississauga, 2012)
3. A. El-Nemr, M. Ahmed, Y. Benmokrane, "Flexural behavior and serviceability of normal- and high-strength concrete beams reinforced with glass fiber-reinforced polymer bars," *ACI Struct. J.* **110**, 1077–1088 (2013)
4. M.M. Kassem, N. Farghaly, Y. Benmokrane, "Evaluation of flexural behavior and serviceability performance of concrete beams reinforced with FRP bars," *J. Compos. Constr.* **15**, 682–695 (2011)
5. O.M. Mostafa, M.K. Rahman, M.M. Al-Zahrani, S.K. Adekunle, M.A. Al-Osta, S.K. Najamuddin, "Flexural behavior and bond coefficient of BFRP reinforced normal and high strength concrete beams," *Constr. Build. Mater.*, **401**, 132896 (2023)
6. S. Mehany, H.M. Mohamed, A. El-Safty, B. Benmokrane, "Bond-dependent coefficient and cracking behavior of lightweight self-consolidating concrete (LWSCC) beams reinforced with glass- and basalt-FRP bars," *Constr. Build. Mater.*, **329**, 127130 (2022)
7. A. El-Nemr, E.A. Ahmed, C. Barris, B. Benmokrane, "Bond-dependent coefficient of glass- and carbon-FRP bars in normal- and high-strength concretes," *Constr. Build. Mater.*, **113**, 77–89 (2016)
8. A. El-Nemr, E.A. Ahmed, A. El-Safty, B. Benmokrane, "Evaluation of the flexural strength and serviceability of concrete beams reinforced with different types of GFRP bars," *Eng. Struct.* **173**, 606–619 (2018)
9. O. Gouda, A. Hassanein, K. Galal, "Experimental and numerical study on the crack width and deflection performance of GFRP reinforced concrete beams," *Eng. Struct.*, **283**, 115721 (2023)
10. V. Benzecry, A. Ruiz Emparanza, F. De Casoy Basalo, A. Nanni, "Bond coefficient, kb, of GFRP bars," *Constr. Build. Mater.*, **292**, 123380 (2021).
11. H.L. Dong, W. Zhou, Z. Wang, "Flexural performance of concrete beams reinforced with FRP bars grouted in corrugated sleeves," *Compos. Struct.*, **215**, 49–59 (2019)

12. B. McCallum, “Experimental evaluation of the bond dependent coefficient and parameters which influence crack width in GFRP reinforced concrete,” M.A.Sc. thesis, Dalhousie University, Canada (2013)
13. P. Vincent, E. Ahmed, B. Benmokrane, “Characterization of basalt fiber-reinforced polymer (BFRP) reinforcing bars for concrete structures,” *3rd Specialty Conference on Material Engineering & Applied Mechanics* (2013).
14. C. Kassem, A.S. Farghaly, B. Benmokrane, “Evaluation of flexural behavior and serviceability performance of concrete beams reinforced with FRP bars,” *J. Compos. Constr.*, **15**(5), 682–695 (2011)